Adsorption Isotherms of Aspartame on Commercial and Chemically Modified Divinylbenzene−Styrene Resins at Different Temperatures

L. Fernando Bautista, José Pinilla, José Aracil, and Mercedes Martínez*

Department of Chemical Engineering, Universidad Complutense de Madrid, Ciudad Universitaria, 28040 Madrid, Spain

The equilibria of adsorption of aspartame in an aqueous solution on a commercial resin and three chemically modified Amberlite XAD-2 resins were measured at different temperatures within the range (0 to 35) °C. The functional groups, introduced by nucleophilic substitution in the aromatic rings of the divinylbenzene−styrene matrix, were bromine (−Br), bromoethyl (−CH_2CH_2Br), and chloromethyl (−CH_2-Cl). All of the isotherms showed a nonlinear and favorable shape with decreasing adsorption capacity as the temperature increased. The chloromethylated resin, and, to a lesser degree, the bromoethylated resin, increased the adsorption capacity for aspartame compared to Amberlite XAD-2. At 35 °C, the chloromethyl resin showed up to a 280% higher saturation capacity than the commercial adsorbent. The experimental equilibrium data were fitted to the Langmuir, Freundlich, Langmuir−Freundlich, Redlich−Peterson, and Toth models. Toth and Langmuir−Freundlich isotherms provided very good fittings for all of the resins over the temperature range studied, whereas the Langmuir and Redlich−Peterson equations were less accurate, although the average errors were, in general, below 10% with respect to the measured values.

Introduction

Aspartame (α-L-aspartyl-L-phenylalanine methyl ester) is the methyl ester of a dipeptide composed of L-aspartic acid and L-phenylalanine. Because it is up to 150−200 times sweeter than sucrose[1] and because of its absence of nutritional supply, aspartame is widely used in low-calorie diets and products and by patients suffering from diseases such as, for instance, diabetes. The production of aspartame was originally achieved by chemical synthesis;[2−5] however, newer and more advantageous methods based on fermentation[6,7] and biotransformation with immobilized thermolysin[8,9] have been developed. Because of the applications of aspartame in the food and pharmaceutical industry, a high-purity product is required to fulfill the standard specifications. For this purpose, adsorption operations are routinely and successfully employed by these industries in the downstream processing of a large variety of products with different chemical properties and fields of application.[10,11]

The inclusion of adsorption and chromatographic steps within the flowsheet of a biotechnology process requires the development of high-capacity and -selectivity adsorbents, allowing the operation to run at the mildest possible conditions so that the stability of the target compound is not compromised and the economic viability of the process is achieved. Because of their adequate physical properties, adsorption capacity, and relatively low cost, the polymeric divinylbenzene−styrene (DVB−S) resins are employed by the food and pharmaceutical industries for the purification of amino acids and peptides,[12] antibiotics such as thienamicin,[13] vitamin B_{12},[14] prostaglandine,[15] etc. Moreover, the chemically modified adsorbents of this type have shown to exhibit significant improvements in the capacity and selectivity for some compounds such as cephalosporin C,[16] amino acids, and peptides.[17]

* Corresponding author. Fax: (+34) 91 394 4167. E-mail: mmr1@quim.ucm.es.

Despite the fact that downstream processing in biotechnology commonly uses purification processes based on adsorption, there is a lack of experimental data for many adsorbate/adsorbent systems. This makes the design and scale-up of downstream processing an empirical and time-consuming task. The availability of equilibrium data and reliable mathematical isotherm expressions describing experimental systems, which can be included in robust phenomenological models, would help to develop more rational and systematic methods to design and scale-up the adsorption processes.

In the present work, the chemical modification of Amberlite XAD-2 was performed with the aim of improving its capacity for the adsorption of aspartame. Furthermore, the adsorption equilibria of aspartame on the commercial and three modified resins were measured at different temperatures. In addition, the experimental data were fitted to several nonlinear isotherm models used to describe the adsorption equilibrium in the liquid phase.

Experimental Section

Adsorbate and Chemicals. Aspartame was purchased from Sigma Chemical Co. (St. Louis, IL). Adsorption experiments were carried out using a 0.1 M HCl/NaCl buffer at pH 2.8 prepared with analytical-grade hydrochloric acid (Merck, Darmstadt, Germany) and sodium chloride (Panreac Química, Barcelona, Spain). All of the adsorption solutions were filtered through 0.80 μm of cellulose ester membranes (AAWP 047 00, Millipore, Bedford, MA) prior to use.

All of the chemicals used for the functionalization methods of Amberlite XAD-2 were supplied by BDH Chemicals (Poole, U.K.) with reagent-grade quality. Among them, carbon tetrachloride, benzene, and chloroform were desiccated with $MgSO_4$ and filtered before they were used as solvents in the functionalization reactions.

10.1021/je010325a CCC: $22.00
Published on Web 04/17/2002

Adsorbents. Amberlite XAD-2 was supplied by Rohm and Haas España (Barcelona, Spain). The adsorbent beads were treated with methanol in a Soxhlet extractor system to remove the monomer trapped inside the pores during the synthesis process. The resin was sieved and the fraction of 0.25−0.50 mm collected for further treatment and use. Then, the adsorbent was thoroughly washed, sequentially, with 1 M NaOH, distilled water, 1 M HCl, distilled water, dimethylformamide, methanol, and distilled water again. Finally, it was dried at 100 °C under reduced pressure. The pretreated commercial resin was used for the further synthesis of the following functionalized adsorbents.

XAD-2-Br modified resin was prepared by bromination of Amberlite XAD-2 with iron(III) chloride as the catalyst in a batch stirred tank.[18] The reaction medium was a solution of bromine in carbon tetrachloride as the solvent. The resin beads and the catalyst were suspended, for 24 h, in this solution in the absence of light in order to avoid secondary reactions. The slurry was filtered and the resin repeatedly washed with acetone until the bromine color disappeared. Then, the resin was washed with dioxane/water (2:1) and, finally, with acetone again. The beads were dried at 100 °C under reduced pressure.

Bromoethylated Amberlite XAD-2, i.e., XAD-2-CH_2CH_2-Br, was produced by nucleophilic reaction in a batch stirred tank too.[19] In this case, the reaction took place between Amberlite XAD-2 and 1,2-dibromoethane in a dry benzene solvent medium. The reaction was stirred for 2.5 h, and then the slurry was filtered, washed, and dried as described for the brominated resin above.

The chloromethylation of Amberlite XAD-2 was performed as follows. The commercial resin was immersed in chloroform at 25 °C for 1 h to allow the beads to swell. Then, the slurry was cooled to 0 °C, and a cold solution of anhydrous tin tetrachloride in chloromethyl methyl ester was added, keeping the suspension agitated for 30 min. After filtration and collection of the adsorbent, the beads were sequentially washed with dioxane/3 M HCl of decreasing volume ratio, starting with 3:1 and ending with pure dioxane. Then, the resin was rinsed with methanol and dried at 100 °C under reduced pressure.[20]

Equilibrium Experiments. Experiments leading to the determination of the adsorption equilibrium isotherms were conducted in batch operation in 250-mL glass flasks where the aspartame solutions were contacted with the corresponding resin. The suspension was stirred with a marine-type impeller fitted to an IKA RW-20 motor (Janke & Kunkel, Staufen, Germany) at 200 rpm. The adsorption vessel was immersed in a Heto DT1 CB-8-30e thermostatic bath (Heto-Holten, Allerød, Denmark) to keep the temperature at the selected value during the development of the experiment.

Samples were withdrawn at regular intervals, and the concentration of aspartame in the adsorption solution was measured by high-performance liquid chromatography (HPLC). This was repeated until a constant concentration was achieved. The concentration of aspartame adsorbed on the modified resin was estimated by mass balance according to the following equation:

$$q = (C_0 - C_E)V/m \qquad (1)$$

where q is the concentration of aspartame on the adsorbed phase, expressed as the amount of aspartame per unit amount of resin (dry basis), C_0 and C_E are respectively the initial and equilibrium concentrations of aspartame in the bulk liquid solution, V is the volume of the adsorption solution, and m is the amount of adsorbent.

Table 1. Physicochemical Properties of the Adsorbents

	XAD-2	XAD-2-Br	XAD-2-$(CH_2)_2$Br	XAD-2-CH_2Cl
porosity	0.45	0.45	0.46	0.45
pore volume (cm^3/g)	0.69	0.49	0.50	0.50
surface area (m^2/g)	312	168	168	143
density (g/cm^3)	0.68	0.57	0.60	0.59
pore size (Å)	88	118	119	142
C (% wt)	91.3	63.5	67.4	85.2
H (% wt)	8.7	6.0	6.4	8.1
Br (% wt)		30.5	26.2	
Cl (% wt)				6.7

Analytical and Characterization Methods. Quantification of the aspartame concentration was carried out by HPLC in a HP-1050 series chromatograph (Hewlett-Packard, Avondale, PA) using a stainless steel column (200 mm × 2.1 mm i.d.). The column was packed with Amberlite XAD-2 with an average particle size of 37 μm. The concentration of aspartame was monitored by the ultraviolet detector at 254 nm and quantified using the corresponding calibration curve.

The physical characterization of the adsorbents (Table 1) was performed in an ASAP 2000 equipment (Micromeritics Instruments Corp., Northcross, GA). The surface area was determined by the Brunauer−Emmett−Teller adsorption isotherm and the pore volume by applying the adsorption/desorption Bopp−Jancso−Heinzinger method.

The atomic composition (C, H, Br, and Cl) of the resins was carried out by elemental analysis, and the results are shown in Table 1.

Experimental Uncertainties. The amounts of solutes used for the preparation of the adsorption and buffer solutions were weighed using an A&D analytical balance (A&D Co., Ltd., Tokyo, Japan) with an accuracy of ±0.0001 g and a repeatability of ±0.0002 g. The volume of deionized water for the buffer and adsorption solutions was measured with an uncertainty of lower than 1% in all of the cases. According to this, the uncertainty in the determination of the aspartame concentration in the initial solution was lower than ±0.002 g/L. On the basis of the estimated calibration error for the relationship between the aspartame concentration and peak area, performed by HPLC analysis, the values were reproducible to within ±0.01 g/L. From eq 1, the calculated values of q were estimated to within ±0.002 g/g_{RES}. The temperature was controlled during each experiment to within ±0.1 °C.

Results and Discussion

Experimental Equilibrium Isotherms. The equilibria of adsorption of aspartame on Amberlite XAD-2 and on the three modified Amberlite XAD-2 resins (i.e., XAD-2-Br, XAD-2-CH_2CH_2Br, and XAD-2-CH_2Cl) were measured at (0, 15, 25, and 35) °C (Table 2). From the plot of the experimental isotherms (Figure 1), it was observed that all of the equilibrium isotherms were nonlinear and favorable.

The functionalization process for XAD-2-CH_2Cl and XAD-2-CH_2CH_2Br increased the adsorption capacity for aspartame with respect to the original Amberlite XAD-2 within the whole temperature range studied. The opposite was observed for XAD-2-Br, whose saturation capacity was considerably lower than that of the commercial adsorbent. The improvement in the performance of the methyl chloride resin, compared to Amberlite XAD-2, increased with temperature from a 50% at 0 °C up to 280% at 35 °C. For the ethyl bromide resin, despite the fact that a more moderate

Table 2. Experimental Adsorption Isotherms for Each Resin at Different Temperatures

	0 °C		15 °C		25 °C		35 °C	
	c, g/L	*q*, g/g_{RES}	*c*, g/L	*q*, g/g_{RES}	*c*, g/L	*q*, g/g_{RES}	*c*, g/L	*q*, g/g_{RES}
XAD-2	0.000	0.000	0.000	0.000	0.000	0.000	0.000	0.000
	0.127	0.035	0.193	0.020	0.180	0.020	0.200	0.016
	0.268	0.067	0.350	0.043	0.400	0.030	0.424	0.023
	0.420	0.095	0.520	0.066	0.570	0.050	0.650	0.028
	0.529	0.136	0.800	0.093	0.790	0.060	0.919	0.025
	0.892	0.175	1.124	0.108	1.200	0.069	1.400	0.030
	1.385	0.177	1.614	0.111	1.680	0.070	1.900	0.030
XAD-2-Br	0.000	0.000	0.000	0.000	0.000	0.000	0.000	0.000
	0.140	0.032	0.194	0.016	0.200	0.010	0.200	0.007
	0.354	0.042	0.400	0.025	0.444	0.016	0.455	0.013
	0.580	0.049	0.645	0.030	0.680	0.020	0.690	0.016
	0.812	0.054	0.895	0.034	0.930	0.021	0.950	0.017
	1.264	0.058	1.353	0.038	1.430	0.022	1.440	0.017
	1.750	0.061	1.868	0.038	1.903	0.024	1.940	0.017
XAD-2-$(CH_2)_2$Br	0.000	0.000	0.000	0.000	0.000	0.000	0.000	0.000
	0.108	0.041	0.230	0.058	0.150	0.029	0.210	0.012
	0.185	0.091	0.255	0.071	0.280	0.063	0.419	0.023
	0.305	0.128	0.450	0.086	0.490	0.075	0.554	0.026
	0.550	0.174	0.800	0.118	0.850	0.099	0.650	0.029
	0.811	0.198	1.033	0.134	1.120	0.109	0.902	0.028
	1.250	0.216	1.520	0.138	1.610	0.112	1.450	0.029
							1.900	0.029
XAD-2-CH_2Cl	0.000	0.000	0.000	0.000	0.000	0.000	0.000	0.000
	0.113	0.039	0.087	0.047	0.097	0.044	0.090	0.054
	0.208	0.084	0.160	0.105	0.218	0.081	0.184	0.091
	0.267	0.139	0.260	0.141	0.350	0.115	0.380	0.107
	0.378	0.179	0.420	0.167	0.460	0.155	0.620	0.109
	0.718	0.225	0.780	0.207	0.890	0.176	0.800	0.115
	1.076	0.266	1.259	0.213	1.400	0.173	1.320	0.112

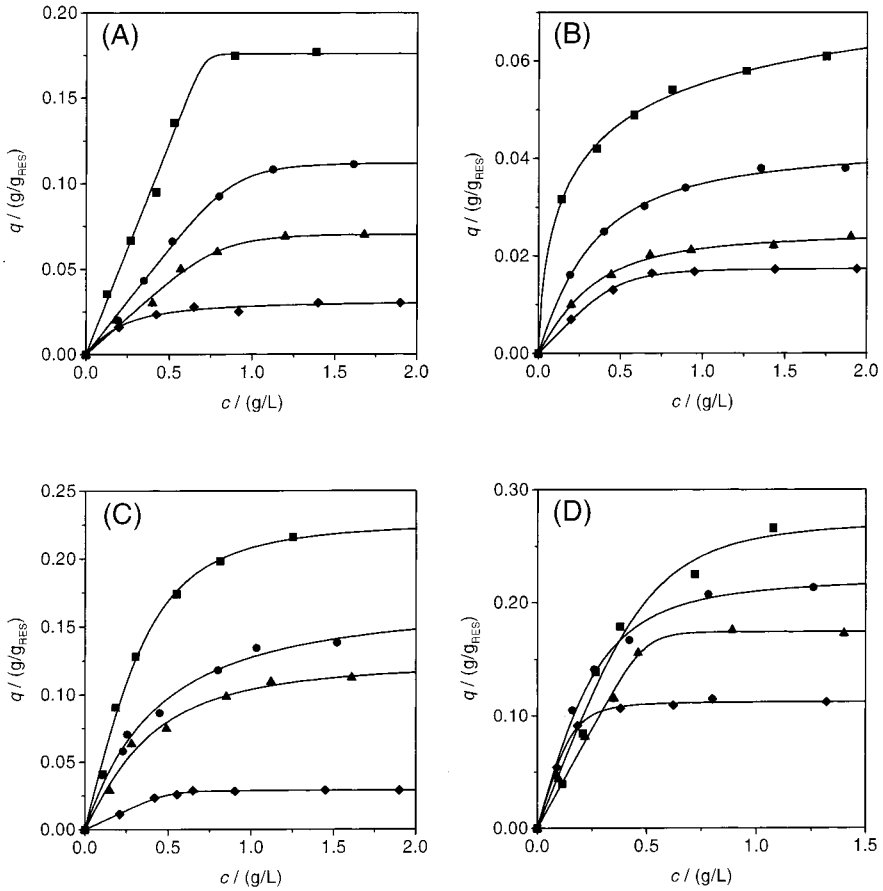

Figure 1. Adsorption isotherms of aspartame on Amberlite XAD-2 (A), XAD-2-Br (B), XAD-2-CH_2CH_2Br (C), and XAD-2-CH_2Cl (D) showing the experimental data (■, 0 °C; ●, 15 °C; ▲, 25 °C; ◆, 35 °C) and their corresponding predicted isotherms from the Toth model (solid lines).

improvement was achieved, up to a 70% increment in the adsorption capacity was measured in the isotherm at 25 °C.

Aspartame, besides its aromatic moiety, also contains chemical groups conferring some polar features. Because the methyl chloride and, to a less extent, the ethyl bromide

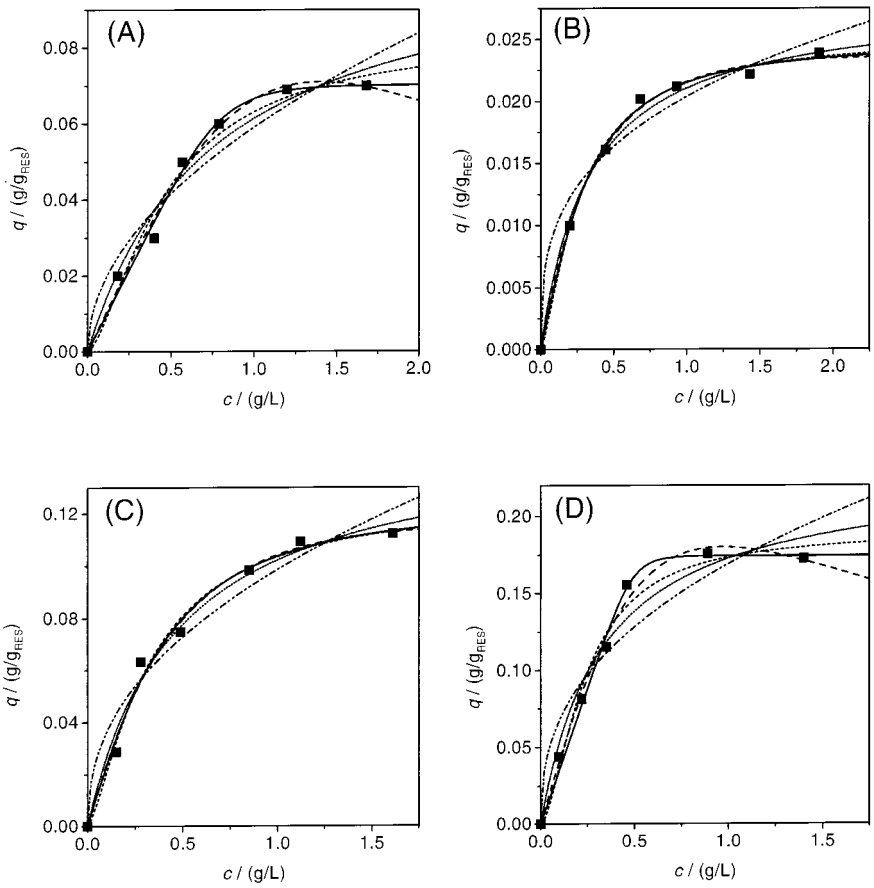

Figure 2. Adsorption isotherms of aspartame at 25 °C on Amberlite XAD-2 (A), XAD-2-Br (B), XAD-2-CH_2CH_2Br (C), and XAD-2-CH_2Cl (D) showing the experimental data (■) and the best-fitting isotherms corresponding to the Langmuir (···), Freundlich (− - - −), Langmuir (−), Freundlich (- - -), Redlich−Peterson (− −), and Toth (—) models.

modified resins are more polar than the original Amberlite XAD-2, the adsorption capacity for aspartame on both adsorbents was improved, even though the surface area (Table 1) was reduced during the functionalization process.

However, despite the fact that XAD-2-Br also had polar characteristics, the above behavior was not followed by this resin. Here, the poorer adsorption capacity for aspartame was probably due to some steric restriction associated with the lack of an alkyl chain in the functional group. As a result of this direct bond between the aromatic ring and the bromine atom in the adsorbent, the aspartame molecule cannot accommodate its polar and nonpolar moieties onto the corresponding DVB−S aromatic matrix and polar functional group of the XAD-2-Br resin.

Isotherm Models. Because of the marked nonlinear behavior of all of the isotherms, at least a two-parameter model must be used to fit the experimental equilibrium data.

The Langmuir isotherm[21] has been commonly used for many different adsorbate/adsorbent systems for both liquid- and gas-phase adsorption with satisfactory results.[22,23] The equation has proved its consistency from both the classical[22] and statistical[24] thermodynamics points of view. It can be written as

$$q = \frac{Q_m bc}{1 + bc} \tag{2}$$

where Q_m is the maximum adsorption capacity, c is the aspartame concentration in the liquid phase inside the pores in equilibrium with q, and b is a model parameter accounting, somehow, for the degree of affinity between the adsorbate and adsorbent.

The second mathematical model used in the present work was the Freundlich isotherm (eq 3). It is also a two-parameter model widely employed not only in gas systems but also in the liquid phase in order to describe the equilibrium of adsorption of aqueous solutions of organic molecules on activated carbon.[25] The Freundlich equation can be expressed as

$$q = k_f \cdot c^{\beta} \tag{3}$$

where k_f and β are temperature-dependent parameters for each adsorption system.

The Freundlich isotherm was first conceived as an empirical model, although it can be derived from the assumption that the surface is composed of "patches", following an exponential decay energy distribution with a Langmuir-type isotherm behavior on each "patch". However, the equation does not account for Henry's law behavior at low surface coverage and for the saturation of the adsorbed phase.

To overcome the last limitation, the Sips isotherm (eq 4), which is a modified Freundlich equation that included the asymptotic saturation effect,[26] has been used. However, it still does not describe adequately the limiting Henry's law region at low concentration. The Sips isotherm is

$$q = \frac{Q_m bc^n}{1 + bc^n} \tag{4}$$

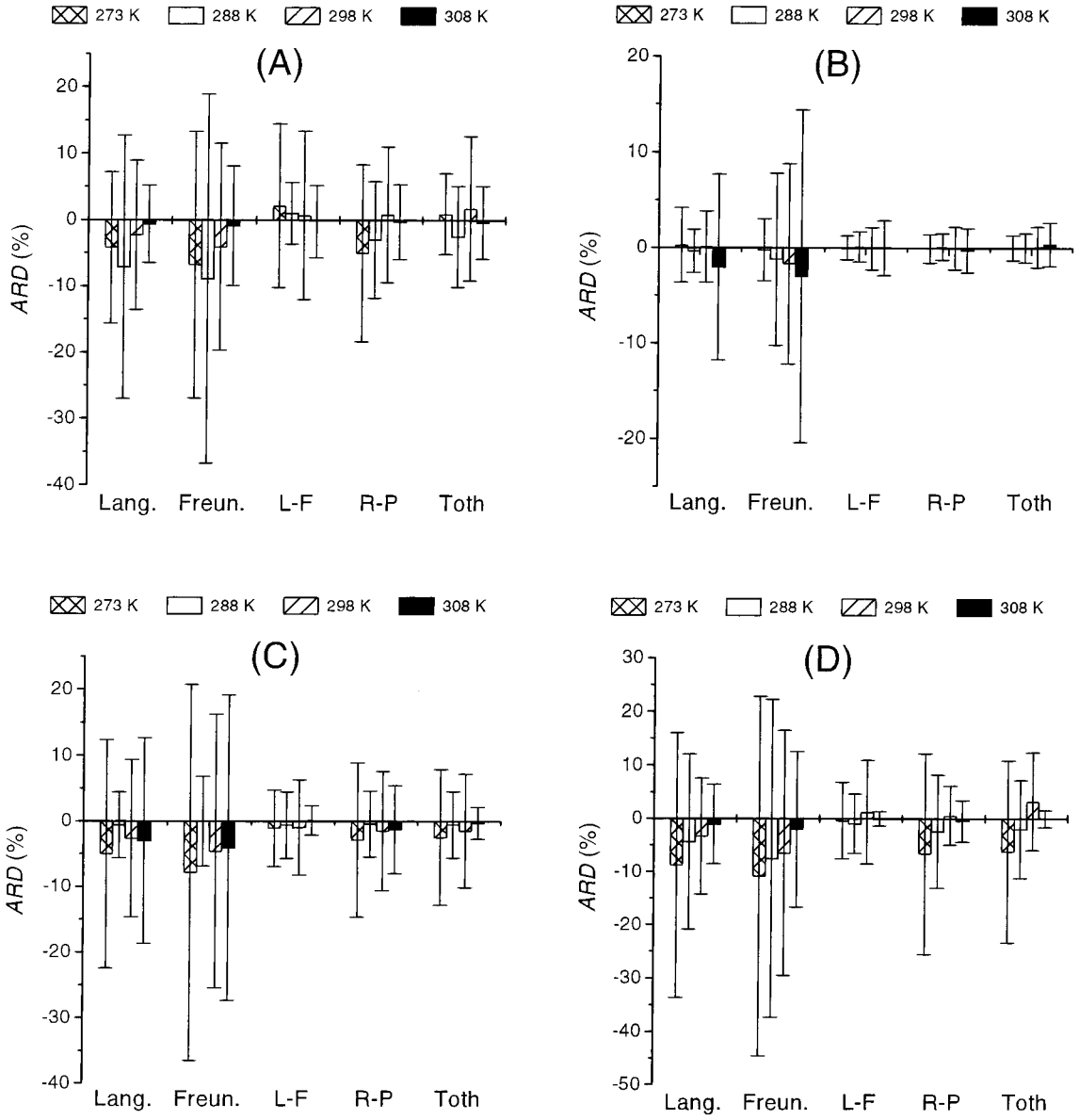

Figure 3. Bar plot of the average residual deviation, ARD, between the experimental data, q_{exp}, and model predictions, q_{mod}, and the corresponding standard deviation for all of the models and temperatures in Amberlite XAD-2 (A), XAD-2-Br (B), XAD-2-CH_2CH_2Br (C), and XAD-2-CH_2Cl (D).

Because of the resemblance of the above equation to the Langmuir isotherm, the Sips model is also known as the Langmuir−Freundlich isotherm.

Redlich and Peterson[27] developed an empirical adsorption equilibrium equation (eq 5) with three parameters that is capable of showing both the linear and saturation behavior within the low and high ends of the isotherm, respectively.

$$q = \frac{Q_m bc}{1 + (bc)^n} \tag{5}$$

This model was first developed to fit the experimental adsorption data in liquid-phase systems, and it has been successfully employed in a large number of adsorption systems,[28] including new applications to molecularly imprinted polymers.[29]

The Toth isotherm[22,23] (eq 6) is another three-parameter isotherm with shape and behavior similar to those of the Redlich−Peterson model. The adsorption equilibrium predicted by the Toth isotherm has a higher slope at low aspartame concentration, that is, before saturation is reached.

$$q = \frac{Q_m bc}{[1 + (bc)^n]^{1/n}} \tag{6}$$

Model Fitting. Each experimental equilibrium isotherm was fitted to the five models described above. Nonlinear regressions of the experimental data to the isotherm models were carried out using the Marquardt algorithm. As an example, Figure 2 shows the results corresponding to the adsorption of aspartame at 25 °C in the four resins studied. To evaluate the goodness of the fitting, the residual deviations (eq 7), RD, between the experimental, q_{exp}, and the calculated, q_{mod}, adsorbed aspartame concentrations were estimated for all of the fittings as follows:

$$\text{RD (\%)} = 100\frac{q_{exp} - q_{mod}}{q_{exp}} \tag{7}$$

Table 3. Comparison of Regression Analysis for Amberlite XAD-2 Showing the Characteristic Parameters of Each Model, Where r^2 Is the Correlation Coefficient and ± Is the Standard Deviation of the Estimated Parameters[a]

isotherm model	parameter	0 °C	15 °C	25 °C	35 °C
Langmuir	Q_m/(g/g$_{RES}$)	0.295 ± 0.048	0.202 ± 0.036	0.107 ± 0.014	0.033 ± 0.002
	b/(L/g)	1.30 ± 0.42	0.90 ± 0.30	1.34 ± 0.40	5.11 ± 1.19
	r^2	0.962	0.968	0.967	0.977
Freundlich	k_f/(L/g)$^\beta$	0.163 ± 0.011	0.092 ± 0.005	0.059 ± 0.003	0.027 ± 0.001
	β	0.56 ± 0.10	0.61 ± 0.11	0.51 ± 0.09	0.23 ± 0.05
	r^2	0.927	0.935	0.937	0.958
Langmuir−Freundlich	Q_m/(g/g$_{RES}$)	0.208 ± 0.028	0.123 ± 0.005	0.083 ± 0.013	0.031 ± 0.003
	b/(L/g)^n	4.60 ± 3.13	4.52 ± 1.06	3.19 ± 2.17	9.55 ± 9.35
	n	1.67 ± 0.42	2.00 ± 0.18	1.51 ± 0.44	1.35 ± 0.56
	r^2	0.974	0.997	0.970	0.974
Redlich−Peterson	Q_m/(g/g$_{RES}$)	0.354 ± 0.010	0.217 ± 0.006	0.142 ± 0.005	0.038 ± 0.012
	b/(L/g)	0.73 ± 0.03	0.59 ± 0.02	0.65 ± 0.07	3.76 ± 2.80
	n	21.8 ± 0.5	2.84 ± 0.45	2.20 ± 0.59	1.06 ± 0.18
	r^2	0.992	0.996	0.983	0.973
Toth	Q_m/(g/g$_{RES}$)	0.176 ± 0.004	0.112 ± 0.003	0.070 ± 0.003	0.031 ± 0.003
	b/(L/g)	1.40 ± 0.05	1.11 ± 0.04	1.22 ± 0.10	3.71 ± 1.58
	n	21.85 ± 0.00	6.27 ± 1.97	5.44 ± 3.60	1.46 ± 0.82
	r^2	0.994	0.997	0.985	0.974

[a] Calculated according to ref 30.

Figure 3 shows the plot of the average residual deviation for each model fitting, ARD, calculated as shown in eq 8,

$$\text{ARD (\%)} = \frac{1}{j}\sum_{i=1}^{j} \text{RD}_i \qquad (8)$$

where j is the number of data measured in each isotherm.

Except for the Freundlich model at 0 °C in XAD-2-CH_2-Cl, all of the average fitting deviations (Figure 3) were lower than 10%; however, the model predictions differed by up to 80% with respect to the corresponding experimental estimated value for some specific data. So, the average fitting uncertainties, although a valid evaluation parameter for the goodness of the fitting, cannot be used as the only selection criteria. To improve the discrimination among different models, the distributions of the residuals were calculated and the degrees of dispersion of the individual uncertainties were included in Figure 3 as the standard deviation of RD for each fitting performed.

The Freundlich model not only gave the poorest fit but also the largest standard deviation at every temperature in all of the resins studied. In addition, it had systematic trends in the residual analysis (data not shown), showing high negative residuals at low concentration levels and high positive residuals in the high loading end of the isotherm.

The other two-parameter model (i.e., the Langmuir isotherm) gave better results than those yielded by the Freundlich isotherm. However, although the average uncertainty was, with a couple of exceptions, lower than 5%, the standard deviation of the residuals was still relatively high, with values above 20% at 0 °C, in the case of Amberlite XAD-2 and XAD-2-CH_2Cl modified resin. The residual analysis for the Langmuir fitting produced a random distribution, without considerable systematic trends, so the Langmuir isotherm can be reasonably considered to be a reliable model for many practical purposes and applications that require one to predict the adsorption equilibrium of aspartame on the DVB−S resins studied in the present work.

As expected, the three-parameter models yielded, in general, better results. However, the Redlich−Peterson equation fitted the experimental data in a fashion similar to that of the Langmuir isotherm. So, from a practical point of view, the higher mathematical complexity of a three-parameter model could not justify the choice of the Redlich−Peterson equation because the simpler two-parameter Langmuir isotherm described the experimental data with similar deviation values. However, the inadequacy of the Redlich−Peterson model in the present work comes from the lack of physical consistency of the predicted curves. The fitting to this model yielded curves with a negative slope in the high-end concentration range of some isotherms (see, for example, Figure 2A,D). This abnormal behavior, without physical meaning, could be due to the wide confidence interval associated with the estimation of the Redlich−Peterson parameters, b and n (Tables 3−6).

The Langmuir−Freundlich and Toth isotherms showed very accurate fittings with a narrow standard deviation of the residuals (Figure 3) in all curves. Although the average and local accuracy of both models were comparable for all of the resins and temperatures, another model feature can be noticed. In fact, the parameter Q_m represents the aspartame saturation capacity of the resin, and it was observed that the Toth equation agreed, with higher precision, with the measured saturation capacity (Table 2) than the Langmuir−Freundlich model. This asymptotic saturation limit, predicted by the Langmuir−Freundlich isotherm, was usually higher than the corresponding experimental value.

Conclusions

The adsorption equilibria of aspartame on a commercial resin and on three chemically modified divinylbenzene−styrene copolymer resins have been studied at different temperatures. All of the experimental isotherms showed a nonlinear and favorable shape, with decreasing capacity as the temperature increased. The adsorption capacity for aspartame of chloromethylated Amberlite XAD-2 was enhanced up to a 280% with respect to the original commercial resin, and that of the bromoethylated resin, up to a 70%. On the other hand, bromination of the original resin yielded a modified adsorbent with poorer adsorption characteristics for aspartame.

The experimental data were fitted to different nonlinear isotherm models. The Langmuir isotherm yielded, in general, satisfactory fittings to the experimental data; however, the errors associated with some measured values were above 20%. Similar fittings were obtained with the Redlich−Peterson equation, but this model seems to be inadequate because it predicts a negative slope in the high-

Table 4. Comparison of Regression Analysis for Amberlite XAD-2-Br Showing the Characteristic Parameters of Each Model, Where r^2 Is the Correlation Coefficient and ± Is the Standard Deviation of the Estimated Parameters[a]

isotherm model	parameter	0 °C	15 °C	25 °C	35 °C
Langmuir	Q_m/(g/g$_{RES}$)	0.066 ± 0.002	0.047 ± 0.001	0.028 ± 0.001	0.021 ± 0.002
	b/(L/g)	5.79 ± 0.67	2.89 ± 0.23	3.00 ± 0.37	3.30 ± 0.87
	r^2	0.994	0.997	0.993	0.970
Freundlich	k_f/(L/g)$^\beta$	0.055 ± 0.001	0.033 ± 0.001	0.020 ± 0.001	0.016 ± 0.001
	β	0.25 ± 0.02	0.33 ± 0.05	0.32 ± 0.05	0.30 ± 0.08
	r^2	0.994	0.973	0.965	0.917
Langmuir−Freundlich	Q_m/(g/g$_{RES}$)	0.083 ± 0.008	0.043 ± 0.002	0.025 ± 0.001	0.018 ± 0.001
	b/(L/g)^n	2.04 ± 0.58	4.11 ± 0.99	5.68 ± 1.69	15.0 ± 5.8
	n	0.61 ± 0.08	1.19 ± 0.13	1.35 ± 0.17	1.98 ± 0.25
	r^2	0.999	0.998	0.996	0.994
Redlich−Peterson	Q_m/(g/g$_{RES}$)	0.041 ± 0.007	0.056 ± 0.004	0.036 ± 0.004	0.033 ± 0.001
	b/(L/g)	16.6 ± 6.9	1.95 ± 0.31	1.87 ± 0.43	1.21 ± 0.14
	n	0.87 ± 0.03	1.13 ± 0.06	1.17 ± 0.10	1.50 ± 0.10
	r^2	0.998	0.998	0.995	0.996
Toth	Q_m/(g/g$_{RES}$)	0.089 ± 0.013	0.042 ± 0.002	0.025 ± 0.001	0.017 ± 0.001
	b/(L/g)	18.3 ± 10.0	2.45 ± 0.23	2.36 ± 0.25	1.96 ± 0.10
	n	0.47 ± 0.11	1.34 ± 0.22	1.62 ± 0.32	3.46 ± 0.62
	r^2	0.999	0.998	0.996	0.998

[a] Calculated according to ref 30.

Table 5. Comparison of Regression Analysis for Amberlite XAD-2-$(CH_2)_2$Br Showing the Characteristic Parameters of Each Model, Where r^2 Is the Correlation Coefficient and ± Is the Standard Deviation of the Estimated Parameters[a]

isotherm model	parameter	0 °C	15 °C	25 °C	35 °C
Langmuir	Q_m/(g/g$_{RES}$)	0.303 ± 0.023	0.186 ± 0.010	0.149 ± 0.010	0.035 ± 0.003
	b/(L/g)	2.23 ± 0.40	2.16 ± 0.30	2.17 ± 0.41	3.93 ± 1.36
	r^2	0.986	0.992	0.984	0.937
Freundlich	k_f/(L/g)$^\beta$	0.209 ± 0.012	0.123 ± 0.004	0.099 ± 0.004	0.027 ± 0.002
	β	0.49 ± 0.07	0.45 ± 0.06	0.44 ± 0.07	0.26 ± 0.09
	r^2	0.949	0.971	0.954	0.871
Langmuir−Freundlich	Q_m/(g/g$_{RES}$)	0.234 ± 0.009	0.174 ± 0.024	0.126 ± 0.012	0.029 ± 0.001
	b/(L/g)^n	7.76 ± 2.10	2.74 ± 1.45	4.71 ± 2.65	46.7 ± 19.3
	n	1.55 ± 0.13	1.10 ± 0.23	1.38 ± 0.30	2.75 ± 0.28
	r^2	0.997	0.990	0.986	0.995
Redlich-Peterson	Q_m/(g/g$_{RES}$)	0.395 ± 0.027	0.214 ± 0.038	0.190 ± 0.029	0.059 ± 0.004
	b/(L/g)	1.31 ± 0.23	1.65 ± 0.60	1.36 ± 0.47	1.19 ± 0.22
	n	1.42 ± 0.22	1.12 ± 0.20	1.26 ± 0.26	1.62 ± 0.20
	r^2	0.992	0.990	0.985	0.983
Toth	Q_m/(g/g$_{RES}$)	0.226 ± 0.014	0.169 ± 0.029	0.124 ± 0.015	0.029 ± 0.001
	b/(L/g)	2.13 ± 0.15	2.07 ± 0.30	1.96 ± 0.29	1.97 ± 0.09
	n	2.14 ± 0.58	1.22 ± 0.48	1.64 ± 0.72	6.22 ± 1.88
	r^2	0.994	0.990	0.985	0.996

[a] Calculated according to ref 30.

Table 6. Comparison of Regression Analysis for Amberlite XAD-2-CH_2Cl Showing the Characteristic Parameters of Each Model, Where r^2 Is the Correlation Coefficient and ± Is the Standard Deviation of the Estimated Parameters[a]

isotherm model	parameter	0 °C	15 °C	25 °C	35 °C
Langmuir	Q_m/(g/g$_{RES}$)	0.444 ± 0.073	0.269 ± 0.017	0.230 ± 0.023	0.126 ± 0.005
	b/(L/g)	1.45 ± 0.45	3.74 ± 0.67	3.05 ± 0.83	10.78 ± 2.21
	r^2	0.966	0.982	0.961	0.980
Freundlich	k_f/(L/g)$^\beta$	0.268 ± 0.019	0.213 ± 0.014	0.169 ± 0.013	0.116 ± 0.007
	β	0.61 ± 0.09	0.39 ± 0.07	0.40 ± 0.09	0.21 ± 0.06
	r^2	0.939	0.929	0.901	0.929
Langmuir−Freundlich	Q_m/(g/g$_{RES}$)	0.277 ± 0.020	0.225 ± 0.009	0.190 ± 0.016	0.113 ± 0.001
	b/(L/g)^n	11.8 ± 7.3	13.1 ± 5.2	10.4 ± 7.4	126.7 ± 54.3
	n	1.98 ± 0.36	1.55 ± 0.18	1.63 ± 0.38	2.05 ± 0.18
	r^2	0.987	0.994	0.975	0.998
Redlich−Peterson	Q_m/(g/g$_{RES}$)	0.520 ± 0.035	0.369 ± 0.039	0.358 ± 0.016	0.178 ± 0.016
	b/(L/g)	0.98 ± 0.21	2.02 ± 0.48	1.18 ± 0.15	4.97 ± 1.07
	n	1.74 ± 0.84	1.31 ± 0.17	1.79 ± 0.26	1.20 ± 0.07
	r^2	0.970	0.989	0.989	0.992
Toth	Q_m/(g/g$_{RES}$)	0.271 ± 0.038	0.221 ± 0.012	0.174 ± 0.005	0.112 ± 0.001
	b/(L/g)	1.79 ± 0.22	3.07 ± 0.32	2.02 ± 0.12	5.68 ± 0.34
	n	3.0 ± 2.4	1.98 ± 0.58	8.3 ± 6.6	2.81 ± 0.49
	r^2	0.974	0.991	0.990	0.998

[a] Calculated according to ref 30.

end concentration range of some isotherms. The Toth and Langmuir−Freundlich equations provided the best fittings in all of the cases, although the Toth model predicted with higher accuracy the saturation capacity of the resin. Although for most practical purposes these fittings can be satisfactorily employed, the thermodynamic consistency of these three-parameter models, unlike the Langmuir isotherm, cannot be assumed.

Literature Cited

(1) Klausner, A. Building for success in phenylalanine. *Biotechnology* **1985**, *3*, 301−307.

(2) Davey, J. M.; Laird, A. H.; Morley, J. S. Polypeptides. Part III. The synthesis of the C-terminal tetrapeptide sequence of gastrin, its optical isomers, and acylated derivatives. *J. Chem. Soc. C* **1966**, 555−566.

(3) Ariyoshi, Y.; Takemoto, T. Process for removing an n-formyl group. Eur. Pat. EP0058063, 1982.

(4) Anderson, G. W. Process of preparing α-L-aspartyl-L-phenylalanine methyl ester. U.S. Patent 3,901,871, 1975.

(5) Bachman, G. L.; Oftedahl, M. L.; Vineyard, B. D. Process for the preparation of α-L-aspartyl-L-phenylalanine alkyl esters. U.S. Patent 3,933,781, 1976.

(6) Yokozeki, K. Preparation of L-aspartyl-L-phenylalanine methyl ester. Jpn. Pat. JP60062998, 1985.

(7) Yokozeki, K.; Kubota, K. Production of L-aspartyl-L-phenylalanine or its methyl ester. Jpn. Pat. JP61035797, 1986.

(8) Nakanishi, K.; Takeuchi, A.; Matsuno, R. Long-term continuous synthesis of Aspartame precursor in a column reactor with an immobilized thermolysin. *Appl. Microbiol. Biotechnol.* **1990**, *32*, 633−636.

(9) Cheetham, P. S. J. Biotransformations: new routes to food ingredients. *Chem. Ind.* **1995**, Apr 3, 265−268.

(10) Takayanagi, H.; Fukuda, J.; Miyata, E. Non-ionic adsorbents in separation processes. In *Downstream processing of natural products*; Verrall, M., Ed.; John Wiley & Sons: Chichester, U.K., 1996; pp 159−177.

(11) El Rassi, Z.; Lee, A. L.; Horváth, C. Reversed-phase and hydrophobic interaction chromatography of peptides and proteins. In *Separation processes in biotechnology*; Asenjo, J. A., Ed.; Marcel Dekker: New York, 1990; pp 447−494.

(12) Iskandarani, Z.; Pietrzyk, D. J. Liquid chromatographic separation of amino acids, peptides, and derivatives on a porous polystyrene−divinylbencene copolymer. *Anal. Chem.* **1981**, *53*, 489−495.

(13) Treiber, L. R.; Gullo, V. P. Process for purifying thienamicin. U.S. Patent 4,198,338, 1978.

(14) Yamanaka, K.; Hikami, S. Separation and recovery of vitamin B_{12} and its derivative. Jpn. Pat. JP2286093, 1990.

(15) Nakajima, I.; Suzaki, K.; Tsuji, M. Method for purifying prostaglandin. Jpn. Pat. JP4112866, 1992.

(16) Martínez, M.; Casillas, J. L.; Aracil, J.; Addo-Yobo, F. Purification of bioproducts using modified resins. Discrimination of adsorbents evaluating breakthrough curves with the method of moments. In *Upstream and downstream processing in biotechnology III*; Technologisch Instituut − K VIV: Amsterdam, The Netherlands, 1991; Vol. 16, pp 3.45−3.51.

(17) Martínez, M.; Carrancio, A.; Casillas, J. L.; Aracil, J. Evaluation of kinetic and thermodynamic parameters of amino acids on modified divinylbenzene−polystyrene resins using a liquid chromatographic technique. *Ind. Eng. Chem. Res.* **1995**, *34*, 4486−4493.

(18) Farrall, M. J.; Fréchet, J. M. J. Bromination and lithiation: two important steps in the functionalization of polystyrene resins. *J. Org. Chem.* **1976**, *41*, 3877−3882.

(19) Martínez, M.; Aracil, J.; Addo-Yobo, F.; Kenney, C. N. Use of brominated polystyrene resin for the adsorption of tryptophan over acidic conditions. *DECHEMA Biotechnology Conference*; VGH: Frankfurt, 1988; Vol. 2, pp 83−90.

(20) Merrifield, R. B. Solid phase peptide synthesis. I. The synthesis of a tetrapeptide. *J. Am. Chem. Soc.* **1963**, *85*, 2149−2154.

(21) Langmuir, I. The adsorption of gases on plane surfaces of glass, mica and platinum. *J. Am. Chem. Soc.* **1918**, *40*, 1361−1404.

(22) Ruthven, D. M. *Principles of adsorption and adsorption processes*; John Wiley & Sons: New York, 1984.

(23) Do, D. D. *Adsorption analysis: Equilibria and kinetics*; Imperial College Press: London, 1998.

(24) Rudzinski, W.; Everett, D. H. *Adsorption of gases on heterogeneous surfaces*; Academic Press: San Diego, 1992.

(25) Al-Duri, B. A review in equilibrium in single and multicomponent liquid adsorption systems. *Rev. Chem. Eng.* **1995**, *11*, 101−143.

(26) Sips, R. Structure of a catalyst surface. *J. Chem. Phys.* **1948**, *16*, 490−495.

(27) Redlich, O.; Peterson, D. L. A useful adsorption isotherm. *J. Phys. Chem.* **1959**, *63*, 1024−1029.

(28) McKay, G.; Al-Duri, B. Extended empirical Freundlich isotherm for binary systems: a modified procedure to obtain the correlation constants. *Chem. Eng. Proc.* **1991**, *29*, 133−138.

(29) Umplebil, R. J.; Baxter, S. C.; Bode, M.; Berch, J. K.; Shah, R. N.; Shimizu, K. D. Application of the Freundlich adsorption isotherm in the chracterization of molecularly imprinted polymers. *Anal. Chim. Acta* **2001**, *435*, 35−42.

(30) Press, W. H.; Teukolsky, S. A.; Vetterling, W. T.; Flannery, B. P. *Numerical recipes in Fortran*; Cambridge University Press: Cambridge, U.K., 1992.

Received for review December 14, 2001. Accepted March 11, 2002.

JE010325A